Reactions of Rhodium and Ruthenium Atoms with Nitrous Oxide: A Combined Matrix Infrared Spectroscopic and Theoretical Study

Ling Jiang and Qiang Xu*

National Institute of Advanced Industrial Science and Technology (AIST), Ikeda, Osaka 563-8577, Japan

Received: February 4, 2009; Revised Manuscript Received: March 23, 2009

Reactions of laser-ablated Rh and Ru atoms with N_2O molecules in excess argon have been investigated using matrix-isolation infrared spectroscopy. Rhodium and ruthenium nitrous oxide complexes, $M(NNO)_x$ ($M = Rh, Ru$; $x = 1, 2$), have been observed and identified on the basis of isotopic shifts, mixed isotopic splitting patterns, and CCl_4-doping experiments. Density functional theory calculations have been performed on the products. The overall agreement between the experimental and calculated vibrational frequencies, relative absorption intensities, and isotopic shifts supports the identification of these species from the matrix infrared spectra. Furthermore, a plausible reaction mechanism for the formation of the products has been proposed.

Introduction

Nitrous oxide (N_2O) is isoelectronic with carbon dioxide (CO_2) but exhibits a global warming potential about 310 times that of CO_2 on a per molecule basis[1] and is responsible for the destruction of the ozone layer in the stratosphere.[2] N_2O also acts as a potentially clean and highly selective oxygen donor for catalytic oxidation processes.[2,3] Much attention has been paid to the catalytic removal of N_2O from industrial exhaust gases. Supported transition metals (i.e., Rh, Co, Ru, Fe, Ni, Pd, and Pt) on oxides and/or zeolites have been widely used in such processes.[4−10] It has been found that $Rh/\gamma\text{-}Al_2O_3$ exhibits high performance of the removal of N_2O.[6,10] Theoretical investigations predict that the rate of N_2O decomposition on Co-ZSM-5 is significantly higher than that on Fe-ZSM-5.[11]

Gas-phase reactions of various metal atoms with N_2O have been extensively investigated both experimentally and theoretically.[12−20] It has been found that the reaction of transition-metal atoms with N_2O leads to N−O bond activation to form the metal oxide and N_2. The reactions were predicted to proceed via the initial formation of a weakly bound complex. Recent studies have shown that the technique of matrix-isolation infrared spectroscopy, combined with quantum chemical calculation, allows the observation of exotic species not accessible from high-temperature typical of traditional approaches.[21,22] Argon matrix investigations of the reactions of laser-ablated Ti, Cr, groups 3, 10, and 13, and lanthanoid metal atoms with N_2O have characterized a series of neutral metal monoxide−dinitrogen and metal nitrous oxide complexes and cationic metal monoxide-dinitrogen complexes.[23−29] Copper and silver chloride−nitrous oxide complexes ClCuNNO and ClAgNNO have also been obtained in the reactions of metal chlorides with nitrous oxide.[30] Herein, we report a combined matrix infrared spectroscopic and theoretical study of the reactions of rhodium and ruthenium atoms with nitrous oxide in excess argon. Infrared spectroscopy coupled with density functional theory calculation provides evidence for the formation of the $M(NNO)_x$ ($M = Rh, Ru$; $x = 1, 2$) complexes.

* To whom correspondence should be addressed. E-mail: q.xu@aist.go.jp.

Experimental and Theoretical Methods

The experiments for laser ablation and matrix-isolation infrared spectroscopy are similar to those previously reported.[31] In short, the Nd:YAG laser fundamental (1064 nm, 10 Hz repetition rate with 10 ns pulse width) was focused on the rotating pure Rh and Ru targets. The laser-ablated Rh and Ru atoms were codeposited with N_2O in excess argon onto a CsI window cooled normally to 4 K by means of a closed-cycle helium refrigerator. Typically, 1−25 mJ/pulse laser power was used. N_2O (99.5%, Taiyo Nippon Sanso Co.), $^{15}N_2O$ (98%, Cambridge Isotopic Laboratories), and $^{14}N_2O + {}^{15}N_2O$ mixtures were used in different experiments. In general, matrix samples were deposited for 30−60 min with a typical rate of 2−4 mmol/h. After sample deposition, IR spectra were recorded on a BIO-RAD FTS-6000e spectrometer at 0.5 cm^{-1} resolution using a liquid nitrogen cooled HgCdTe (MCT) detector for the spectral range of 5000−400 cm^{-1}. Samples were annealed at different temperatures and subjected to broadband irradiation ($\lambda > 250$ nm) using a high-pressure mercury arc lamp (Ushio, 100 W).

Density functional theory (DFT) calculations were performed to predict the structures and vibrational frequencies of the reaction products using the Gaussian 03 program.[32] The B3LYP density functional method was employed.[33] The 6-311+G(d) basis set was used for the N and O atoms,[34] and the scalar-relativistic SDD pseudopotential and basis set were used for the Rh and Ru atoms.[35] Geometries were fully optimized and vibrational frequencies were calculated with analytical second derivatives. Recent investigations have shown that such computational scheme can provide reliable information for metal complexes, such as infrared frequencies, relative absorption intensities, and isotopic shifts.[23−30,36−38]

Results and Discussion

Experiments have been done with nitrous oxide concentrations ranging from 0.02% to 1.0% in excess argon. Typical infrared spectra for the reactions of laser-ablated Rh and Ru atoms with N_2O molecules in excess argon in the selected regions are illustrated in Figures 1−4, and the absorption bands in different isotopic experiments are listed in Table 1. The stepwise annealing and irradiation behavior of the product absorptions

10.1021/jp9010422 CCC: $40.75
Published on Web 04/15/2009

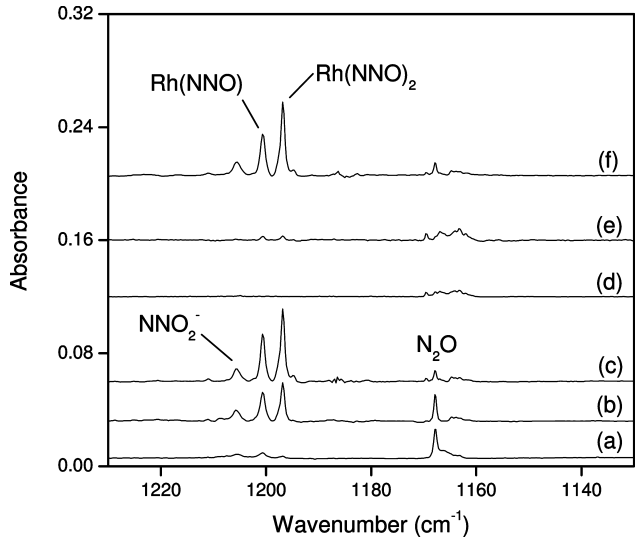

Figure 1. Infrared spectra in the 1220−1140 cm^{-1} region from codeposition of laser-ablated Rh atoms with 0.2% N_2O in Ar at 4 K: (a) spectrum obtained from initial sample deposited for 1 h; (b) spectrum after annealing to 30 K; (c) spectrum after annealing to 35 K; (d) spectrum after 10 min of broadband irradiation; (e) spectrum after annealing to 39 K; (f) spectrum obtained by depositing laser-ablated Rh atoms with 0.2% N_2O + 0.03% CCl_4 in Ar at 4 K for 1 h and annealing to 35 K.

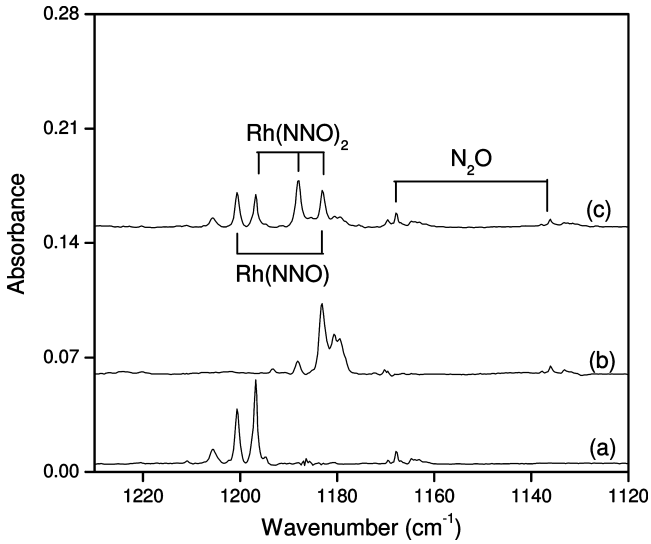

Figure 2. Infrared spectra in the 1220−1120 cm^{-1} region from codeposition of laser-ablated Rh atoms with isotopic N_2O in Ar after annealing to 35 K: (a) 0.2% $^{14}N_2O$; (b) 0.2% $^{15}N_2O$; (c) 0.15% $^{14}N_2O$ + 0.15% $^{15}N_2O$.

is also shown in the figures and will be discussed below. Experiments were also done with different concentrations of CCl_4 serving as an electron scavenger.[36]

Quantum chemical calculations have been carried out for the possible isomers and electronic states of the reaction products. The comparison of the experimental and calculated IR frequencies and isotopic frequency ratios for the products are summarized in Table 1. Figure 5 shows the optimized structures of the $M(NNO)_x$ (M = Rh, Ru; x = 1, 2) complexes. The ground electronic states, point groups, vibrational frequencies, and intensities of the $M(NNO)_x$ (M = Rh, Ru; x = 1, 2) complexes are listed in Table 2. Representatively, molecular orbital depictions of the highest occupied molecular orbitals (HOMO) of the $Rh(NNO)_x$ (x = 1, 2) complexes are illustrated in Figure 6.

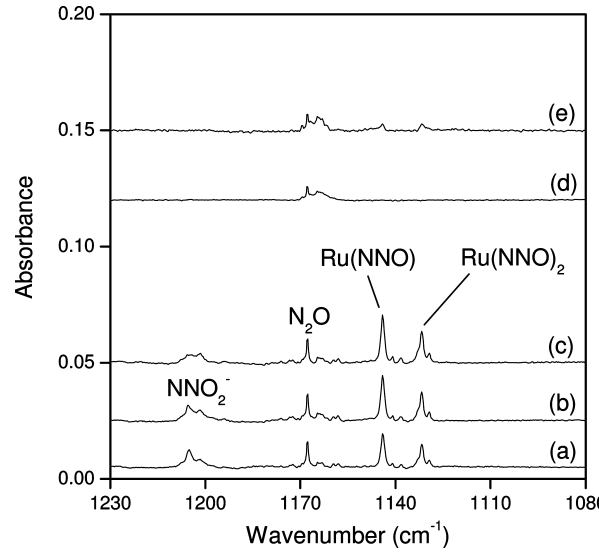

Figure 3. Infrared spectra in the 1230−1080 cm^{-1} region from codeposition of laser-ablated Ru atoms with 0.2% N_2O in Ar at 4 K: (a) spectrum obtained from initial sample deposited for 1 h; (b) spectrum after annealing to 25 K; (c) spectrum after annealing to 30 K; (d) spectrum after 10 min of broadband irradiation; (e) spectrum after annealing to 35 K.

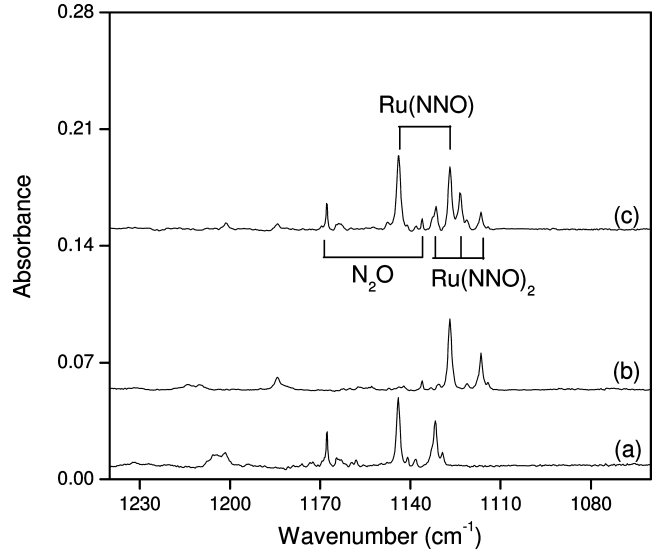

Figure 4. Infrared spectra in the 1230−1080 cm^{-1} region from codeposition of laser-ablated Ru atoms with isotopic N_2O in Ar after annealing to 30 K: (a) 0.2% $^{14}N_2O$; (b) 0.2% $^{15}N_2O$; (c) 0.2% $^{14}N_2O$ + 0.2% $^{15}N_2O$.

TABLE 1: Experimental and Calculated IR Absorptions (in cm^{-1}) and Isotopic Frequency Ratios for the Products

experimental			calculated			
$^{14}N_2O$	$^{15}N_2O$	$^{14}N_2O/^{15}N_2O$	$^{14}N_2O$	$^{15}N_2O$	$^{14}N_2O/^{15}N_2O$	assignment
1200.6	1183.2	1.0147	1249.9	1231.9	1.0146	Rh(NNO)
1196.8	1180.6	1.0137	1245.4	1227.9	1.0143	$Rh(NNO)_2$
1144.0	1126.0	1.0153	1228.4	1210.2	1.0150	Ru(NNO)
1131.7	1116.5	1.0136	1222.9	1205.6	1.0143	$Ru(NNO)_2$

A. M(NNO) (M = Rh, Ru). In the reaction of Rh atoms with N_2O in excess argon, the absorption at 1200.6 cm^{-1} appears weakly during sample deposition, increases sharply after sample annealing, but disappears upon broadband irradiation, and recovers slightly after further annealing to higher temperature (Table 1 and Figure 1). This band shifts to 1183.2 cm^{-1} with

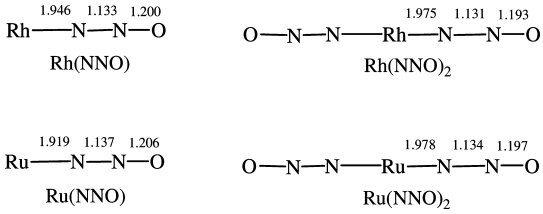

Figure 5. Optimized structures (bond lengths in angstroms, bond angles in degrees) of the $M(NNO)_x$ (M = Rh, Ru; x = 1, 2) complexes.

TABLE 2: Ground Electronic States, Point Groups, Vibrational Frequencies (in cm^{-1}), and Intensities (km/mol) of the N_2O and $M(NNO)_x$ (M = Rh, Ru; x = 1, 2) Complexes

species	elec state	point group	frequency (intensity, mode)
N_2O	$^1\Sigma$	$C_{\infty v}$	2344.6 (401, σ), 1327.7 (69, σ), 580.4 (6 × 2, π)
Rh(NNO)	$^2\Delta$	$C_{\infty v}$	2343.5 (119, σ), 1249.9 (585, σ), 382.3 (5 × 2, π), 308.8 (3, σ), 123.1 (1 × 2, π)
$Rh(NNO)_2$	$^2\Pi$	$D_{\infty h}$	2365.3 (393, σ_u), 2364.8 (0, σ_g), 1300.2 (0, σ_g), 1245.4 (1807, σ_u), 436.2 (8 × 2, π_u), 425.2 (0 × 2, π_g), 326.8 (90, σ_u), 273.9 (0, σ_g), 256.3 (1 × 2, π_u), 129.5 (0 × 2, π_g), 33.4 (0.2 × 2, π_u)
Ru(NNO)	$^3\Delta$	$C_{\infty v}$	2326.1 (92, σ), 1228.4 (694, σ), 356.0 (7, σ), 285.1 (5 × 2, π), 149.0 (0.4 × 2, π)
$Ru(NNO)_2$	$^3\Pi$	$D_{\infty h}$	2342.2 (336, σ_u), 2342.2 (0, σ_g), 1285.3 (0, σ_g), 1222.9 (2117, σ_u), 402.3 (5 × 2, π_u), 376.0 (0 × 2, π_g), 342.8 (93, σ_u), 293.2 (0, σ_g), 282.0 (3 × 2, π_u), 145.7 (0 × 2, π_g), 38.4 (0.4 × 2, π_u)

$^{15}N_2O$ (Table 1 and Figure 2, trace b). The $^{14}N_2O/^{15}N_2O$ isotopic frequency ratio (1.0147) of the 1200.6 cm^{-1} band is slightly smaller than that of the N−O stretching mode of N_2O (1.0155) observed at 1287.5 cm^{-1} in an argon matrix. The band position and the isotopic frequency ratio suggest that this band is due to a N−O stretching mode of a nitrous oxide species. The mixed $^{14}N_2O + ^{15}N_2O$ isotopic spectra (Figure 2, trace c) only provide the sum of pure isotopic bands, which indicates only one N_2O unit is involved in the species.[39] Furthermore, doping with CCl_4 has no effect on this band (Figure 1, trace f), suggesting that the product is neutral.[36] Accordingly, the absorption at 1200.6 cm^{-1} is assigned to the N−O stretching vibrations of the neutral Rh(NNO) complex. Analogous Ru(NNO) complex has been observed at 1144.0 cm^{-1} in an argon matrix (Table 1 and Figures 3 and 4). Recently, the corresponding N−O stretching vibrations of nickel, palladium, and platinum nitrous oxide complexes, M(NNO) (M = Ni, Pd, Pt), have been observed at 1185.5, 1226.8, and 1229.4 cm^{-1} in an argon matrix,[26] respectively.

DFT calculations predict that the Rh(NNO) and Ru(NNO) complexes have linear structures with doublet and triplet ground states (Table 2 and Figure 5), respectively. N_2O bonds in an end-on orientation with the nitrogen-end toward the metal atoms in these complexes (Figure 5). For the Rh(NNO) complex, the N−O stretching vibration is calculated to be 1249.9 cm^{-1} (Table 2). As listed in Table 1, the calculated $^{14}N_2O/^{15}N_2O$ isotopic frequency ratio for the N−O stretching vibration (1.0146) is in accord with experimental value (1.0147). The N−N stretching vibration is calculated to be 2343.5 cm^{-1} (Table 2). With its small intensity (119 km/mol) relative to the N−O stretching vibration (585 km/mol) (Table 2), it is not easy to be observed, consistent with the absence from the present experiment. These agreements between the experimental and calculated vibrational frequencies, relative absorption intensities, and isotopic shifts support the identification of the Rh(NNO) complex from the matrix IR spectra. Similar results has also been obtained for the Ru(NNO) complex (Tables 1 and 2).

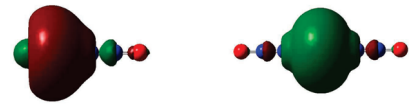

Rh(NNO) $Rh(NNO)_2$

Figure 6. Molecular orbital depictions of the highest occupied molecular orbitals (HOMOs) of the $Rh(NNO)_x$ (x = 1, 2) complexes.

B. $M(NNO)_2$ (M = Rh, Ru). In the Rh + N_2O experiments, the absorption at 1196.8 cm^{-1} that appears weakly during sample deposition, increases sharply after sample annealing, but disappears upon broadband irradiation, and recovers slightly after further annealing to higher temperature (Table 1 and Figure 1). The 1196.8 cm^{-1} band shifts to 1180.6 cm^{-1} with $^{15}N_2O$ (Table 1 and Figure 2, trace b). The $^{14}N_2O/^{15}N_2O$ isotopic frequency ratio (1.0137) of the 1196.8 cm^{-1} band is similar to that of the 1200.6 cm^{-1} band of Rh(NNO), slightly smaller than that of the N−O stretching mode of N_2O (1.0155) observed at 1287.5 cm^{-1} in an argon matrix. The band position and the isotopic frequency ratio imply that the 1196.8 cm^{-1} band is also due to a N−O stretching mode of a nitrous oxide species. In the mixed $^{14}N_2O + ^{15}N_2O$ experiment (Figure 2, trace c), a triplet at 1196.8, 1188.0, and 1180.5 cm^{-1} with approximately 1:2:1 relative intensities is observed, suggesting that two equivalent N_2O subunits are involved in this mode.[39] Furthermore, doping with CCl_4 has no effect on this band (Figure 1, trace f), suggesting that the product is neutral.[36] Accordingly, the absorption at 1196.8 cm^{-1} is assigned to the antisymmetric N−O stretching vibration of the neutral $Rh(NNO)_2$ complex. The ruthenium counterpart is observed at 1131.7 cm^{-1} in an argon matrix (Table 1 and Figures 3 and 4). Analogously, the corresponding antisymmetric N−O stretching vibrations of neutral $M(NNO)_2$ (M = Ni, Pd) complexes in solid argon have been observed at 1150.3 and 1226.3 cm^{-1},[26] respectively.

The assignment is supported by the DFT calculations, which predict the $Rh(NNO)_2$ and $Ru(NNO)_2$ complexes to have linear structures with doublet and triplet ground states (Table 2 and Figure 5), respectively. It can be seen from Figure 5 that these complexes have structures with the terminal N atom of N_2O bound to the metal atoms. For the $Rh(NNO)_2$ complex, the antisymmetric N−O stretching vibration is calculated to be 1245.4 cm^{-1} (Table 2). The calculated $^{14}N_2O/^{15}N_2O$ isotopic frequency ratio for the antisymmetric N−O stretching vibration (1.0143) is consistent with the experimental value (1.0137) (Table 1). The antisymmetric N−N stretching vibration of the $Rh(NNO)_2$ complex is calculated to be 2365.3 cm^{-1} (Table 3). With its small intensity (393 km/mol) relative to the antisymmetric N−O stretching vibration (1807 km/mol) (Table 3), it is not easy to be observed, consistent with the absence from the present experiments. For the $Ru(NNO)_2$ complex, the overall agreement between the experimental and calculated vibrational frequencies, relative absorption intensities, and isotopic shifts has also been obtained (Tables 1 and 2), which supports the identification of this species from the matrix infrared spectra.

It is noted that the absorptions of the N−N stretching vibrational modes in the ORhNN and ORuNN complexes are predicted to be 2345.0 and 2237.1 cm^{-1} (not shown here),

respectively, which are very close to the N−N stretching vibrational frequency of N_2O. Therefore, the adsorption of inserted ORhNN and ORuNN species may be overlapped by the broad absorptions of N_2O and cannot be observed in the present experiments.

C. Reaction Mechanism and Bonding Consideration. On the basis of the behavior of sample annealing and irradiation, together with the observed species and calculated stable isomers, a plausible reaction mechanism can be proposed as follows. Under the present experimental conditions, the $M(NNO)_x$ (M = Rh, Ru; $x = 1, 2$) complexes are the primary products after sample annealing (Figures 1 and 3), which are formed from the reactions of metal atoms with N_2O (reactions 1−3 and 5−7). These association reactions are predicted to be exothermic. It can be found that the formation of the Ru(NNO) and $Ru(NNO)_2$ complexes (reactions 5−7) is predicted to be more energetically favorable than that of the corresponding rhodium complexes (reactions 1−3). Furthermore, the isomerizations of M(NNO) to OMNN (M = Rh, Ru) are calculated to be exothermic by 48.7 kcal/mol for Rh (reaction 4) and 62.5 kcal/mol for Ru (reaction 8), respectively. As mentioned above, the absorptions of the N−N stretching vibrational modes of the ORhNN and ORuNN complexes may be overlapped by the broad absorptions of N_2O.

$$Rh(^2F)+N_2O(^1\Sigma)\rightarrow Rh(NNO)(^2\Delta)$$
$$\Delta E = -22.2 \text{ kcal/mol} \quad (1)$$

$$Rh(^4F)+N_2O(^1\Sigma)\rightarrow Rh(NNO)(^2\Delta)$$
$$\Delta E = -10.4 \text{ kcal/mol} \quad (2)$$

$$Rh(NNO)(^2\Delta)+N_2O(^1\Sigma)\rightarrow Rh(NNO)_2(^2\Pi)$$
$$\Delta E = -25.7 \text{ kcal/mol} \quad (3)$$

$$Rh(NNO)(^2\Delta)\rightarrow ORhNN(^4A'')$$
$$\Delta E = -48.7 \text{ kcal/mol} \quad (4)$$

$$Ru(^3F)+N_2O(^1\Sigma)\rightarrow Ru(NNO)(^3\Delta)$$
$$\Delta E = -33.9 \text{ kcal/mol} \quad (5)$$

$$Ru(^5F)+N_2O(^1\Sigma)\rightarrow Ru(NNO)(^3\Delta)$$
$$\Delta E = -12.5 \text{ kcal/mol} \quad (6)$$

$$Ru(NNO)(^3\Delta)+N_2O(^1\Sigma)\rightarrow Ru(NNO)_2(^3\Pi)$$
$$\Delta E = -30.2 \text{ kcal/mol} \quad (7)$$

$$Ru(NNO)(^3\Delta)\rightarrow ORuNN(^3A'')$$
$$\Delta E = -62.5 \text{ kcal/mol} \quad (8)$$

It is noted that the ground-state N_2O molecule has an electron configuration of $(1\sigma)^2(2\sigma)^2(3\sigma)^2(4\sigma)^2(5\sigma)^2(6\sigma)^2(1\pi)^4(7\sigma)^2(2\pi)^4(3\pi)^0$. Taking the $Rh(NNO)_x$ ($x = 1, 2$) species as an example for the bonding analysis, the highest occupied molecular orbitals (HOMOs) of $Rh(NNO)_x$ ($x = 1, 2$) are σ-type bonds (Figure 6), which comprise the synergic donation between 7σ orbital of N_2O and a vacant metal orbital with σ symmetry. This implies that the 7σ orbital of N_2O is the principle donor orbital, whereas the 2π orbital is less important in donation in the linear $Rh(NNO)_x$ ($x = 1, 2$) structure.

Previous investigations show that metal oxide molecules are the major products in the reactions of N_2O with metal atoms in the gas phase.[12−20] However, it has been found from the matrix experiments (in the condensed phase) that the yields of the rhodium and ruthenium nitrous oxide complexes, $M(NNO)_x$ (M = Rh, Ru; $x = 1, 2$), are larger than those of the RhO and RuO molecules. This suggests the reactivity of gas-phase metal atoms toward N_2O is quite different from that of condensed-phase metal atoms.

Conclusions

Reactions of laser-ablated rhodium and ruthenium atoms with nitrous oxide molecules in excess argon have been investigated using matrix-isolation infrared spectroscopy and density functional theory calculation. In the Rh + N_2O experiments, the absorption at 1200.6 cm^{-1} is assigned to the N−O stretching vibration of the neutral Rh(NNO) complex and the absorption at 1196.8 cm^{-1} is assigned to the antisymmetric N−O stretching vibration of the neutral $Rh(NNO)_2$ complex on the basis of the results of the isotopic substitution, the N_2O concentration change, and CCl_4-doping experiments. Analogous $Ru(NNO)_x$ ($x = 1, 2$) complexes have also been observed in the Ru reaction. The N−N stretching vibrational frequencies of the ORhNN and ORuNN complexes are predicted to be very close to that of N_2O and may be overlapped by the broad absorptions of N_2O. Density functional theory calculations have been performed on these species, which support the experimental assignments of the infrared spectra.

Acknowledgment. This work was supported by AIST and a Grant-in-Aid for Scientific Research (B) (Grant No. 17350012) from the Ministry of Education, Culture, Sports, Science, and Technology (MEXT) of Japan. L.J. is grateful to the Japan Society for the Promotion of Science (JSPS) for a postdoctoral fellowship.

References and Notes

(1) Trogler, W. C. *Coord. Chem. Rev.* **1999**, *187*, 303.
(2) Kapteijn, F.; Rodriguez-Mirasol, J.; Moulijn, J. A. *Appl. Catal., B* **1996**, *9*, 25.
(3) Dandekar, A.; Vannice, M. A. *Appl. Catal., B* **1999**, *22*, 179. Burch, R.; Daniells, S. T.; Breen, J. P.; Hu, P. *J. Catal.* **2004**, *224*, 252.
(4) Centi, G.; Dall'Olio, L.; Perathoner, S. *Appl. Catal., A* **2000**, *194/195*, 79.
(5) Oi, J.; Obuchi, A.; Bamwenda, G. R.; Ogata, A.; Yagita, H.; Kushiyama, S.; Mizuno, K. *Appl. Catal., B* **1997**, *12*, 277.
(6) Haber, J.; Machej, T.; Janas, J.; Nattich, M. *Catal. Today* **2004**, *90*, 15.
(7) Pérez-Ramirez, J.; Kapteijn, F.; Mul, G.; Moulijn, J. A. *J. Catal.* **2002**, *208*, 211.
(8) Wacław, A.; Nowińska, K.; Schwieger, W.; Zielińska, A. *Catal. Today* **2004**, *90*, 21.
(9) da Cruz, R. S.; Mascarenhas, A. J. S.; Andrade, H. M. C. *Appl. Catal., B* **1998**, *18*, 223.
(10) Doi, K.; Wu, Y. Y.; Takeda, R.; Matsunami, A.; Arai, N.; Tagawa, T.; Goto, S. *Appl. Catal., B* **2001**, *35*, 43.
(11) Ryder, J. A.; Chakraborty, A. K.; Bell, A. T. *J. Phys. Chem. B* **2002**, *106*, 7059.
(12) Armentrout, P. B.; Halle, L. F.; Beauchamp, J. L. *J. Chem. Phys.* **1982**, *76*, 2449.
(13) Ritter, D.; Weisshaar, J. C. *J. Phys. Chem.* **1989**, *93*, 1576.
(14) Ritter, D.; Weisshaar, J. C. *J. Phys. Chem.* **1990**, *94*, 4907.
(15) Futerko, P. M.; Fontijn, A. *J. Chem. Phys.* **1991**, *95*, 8065, and references therein.
(16) Futerko, P. M.; Fontijn, A. *J. Chem. Phys.* **1992**, *97*, 3861.
(17) Futerko, P. M.; Fontijn, A. *J. Chem. Phys.* **1993**, *98*, 7004.
(18) Campbell, M. L. *J. Chem. Soc., Faraday Trans.* **1998**, *94*, 1687, and references therein.
(19) Stirling, A. *J. Phys. Chem. A* **1998**, *102*, 6565. Stirling, A. *J. Am. Chem. Soc.* **2002**, *124*, 4058.
(20) Campbell, M. L.; Kolsch, E. J.; Hooper, K. L. *J. Phys. Chem. A* **2000**, *104*, 11147.
(21) For example, see: Xu, C.; Manceron, L.; Perchard, J. P. *J. Chem. Soc., Faraday Trans* **1993**, *89*, 1291. Bondybey, V. E.; Smith, A. M.; Agreiter, J. *Chem. Rev.* **1996**, *96*, 2113. Fedrigo, S.; Haslett, T. L.; Moskovits, M. *J. Am. Chem. Soc.* **1996**, *118*, 5083. Khriachtchev, L.; Pettersson, M.; Runeberg, N.; Lundell, J.; Rasanen, M. *Nature (London)* **2000**, *406*, 874. Himmel, H. J.; Manceron, L.; Downs, A. J.; Pullumbi, P.

J. Am. Chem. Soc. **2002**, *124*, 4448. Li, J.; Bursten, B. E.; Liang, B.; Andrews, L. *Science* **2002**, *295*, 2242. Andrews, L.; Wang, X. *Science* **2003**, *299*, 2049.

(22) Zhou, M. F.; Tsumori, N.; Li, Z.; Fan, K.; Andrews, L.; Xu, Q. *J. Am. Chem. Soc.* **2002**, *124*, 12936. Zhou, M. F.; Xu, Q.; Wang, Z.; Schleyer, P. v. R. *J. Am. Chem. Soc.* **2002**, *124*, 14854. Jiang, L.; Xu, Q. *J. Am. Chem. Soc.* **2005**, *127*, 42. Xu, Q.; Jiang, L.; Tsumori, N. *Angew. Chem., Int. Ed.* **2005**, *44*, 4338. Jiang, L.; Xu, Q. *J. Am. Chem. Soc.* **2005**, *127*, 8906. Jiang, L.; Xu, Q. *J. Am. Chem. Soc.* **2006**, *128*, 1394 (Addition and Correction).

(23) Chertihin, G. V.; Andrews, L. *J. Phys. Chem.* **1994**, *98*, 5891.

(24) Zhou, M. F.; Zhang, L. N.; Qin, Q. Z. *J. Phys. Chem. A* **2001**, *105*, 6407.

(25) Zhou, M. F.; Wang, G. J.; Zhao, Y. Y.; Chen, M. H.; Ding, C. F. *J. Phys. Chem. A* **2005**, *109*, 5079.

(26) Jin, X.; Wang, G. J.; Zhou, M. F. *J. Phys. Chem. A* **2006**, *110*, 8017.

(27) Wang, G. J.; Zhou, M. F. *Chem. Phys.* **2007**, *342*, 90.

(28) Jiang, L.; Xu, Q. *J. Phys. Chem. A* **2008**, *112*, 6289.

(29) Jiang, L.; Xu, Q. *J. Phys. Chem. A* **2008**, *112*, 8696.

(30) Wang, G. J.; Jin, X.; Chen, M. H.; Zhou, M. F. *Chem. Phys. Lett.* **2006**, *420*, 130.

(31) Burkholder, T. R.; Andrews, L. *J. Chem. Phys.* **1991**, *95*, 8697. Zhou, M. F.; Tsumori, N.; Andrews, L.; Xu, Q. *J. Phys. Chem. A* **2003**, *107*, 2458. Jiang, L.; Xu, Q. *J. Chem. Phys.* **2005**, *122*, 034505. Jiang, L.; Teng, Y. L.; Xu, Q. *J. Phys. Chem. A* **2006**, *110*, 7092.

(32) Frisch, M. J.; Trucks, G. W.; Schlegel, H. B.; Scuseria, G. E.; Robb, M. A. Cheeseman, J. R.; Montgomery, J. A., Jr.; Vreven, T.; Kudin, K. N.; Burant, J. C.; Millam, J. M.; Iyengar, S. S.; Tomasi, J.; Barone, V.; Mennucci, B.; Cossi, M.; Scalmani, G.; Rega, N.; Petersson, G. A.; Nakatsuji, H.; Hada, M.; Ehara, M.; Toyota, K.; Fukuda, R.; Hasegawa, J.; Ishida, M.; Nakajima, T.; Honda, Y.; Kitao, O.; Nakai, H.; Klene, M.; Li, X.; Knox, J. E.; Hratchian, H. P.; Cross, J. B.; Adamo, C.; Jaramillo, J.; Gomperts, R.; Stratmann, R. E.; Yazyev, O.; Austin, A. J.; Cammi, R.; Pomelli, C.; Ochterski, J. W.; Ayala, P. Y.; Morokuma, K.; Voth, G. A.; Salvador, P.; Dannenberg, J. J.; Zakrzewski, V. G.; Dapprich, S.; Daniels, A. D.; Strain, M. C.; Farkas, O.; Malick, D. K.; Rabuck, A. D.; Raghavachari, K.; Foresman, J. B.; Ortiz, J. V.; Cui, Q.; Baboul, A. G.; Clifford, S.; Cioslowski, J.; Stefanov, B. B.; Liu, G.; Liashenko, A.; Piskorz, P.; Komaromi, I.; Martin, R. L.; Fox, D. J.; Keith, T.; Al-Laham, M. A.; Peng, C. Y.; Nanayakkara, A.; Challacombe, M.; Gill, P. M. W.; Johnson, B.; Chen, W.; Wong, M. W.; Gonzalez, C.; Pople, J. A. *Gaussian 03*, revision B.04; Gaussian, Inc.: Pittsburgh, PA, 2003.

(33) Lee, C.; Yang, E.; Parr, R. G. *Phys. Rev. B* **1988**, *37*, 785. Becke, A. D. *J. Chem. Phys.* **1993**, *98*, 5648.

(34) Krishnan, R.; Binkley, J. S.; Seeger, R.; Pople, J. A. *J. Chem. Phys.* **1980**, *72*, 650. McLean, A. D.; Chandler, G. S. *J. Chem. Phys.* **1980**, *72*, 5639.

(35) Andrae, D.; Haeussermann, U.; Dolg, M.; Stoll, H.; Preuss, H. *Theor. Chim. Acta* **1990**, *77*, 123.

(36) Zhou, M. F.; Andrews, L.; Bauschlicher, C. W., Jr. *Chem. Rev* **2001**, *101*, 1931.

(37) Andrews, L.; Citra, A. *Chem. Rev.* **2002**, *102*, 885.

(38) Himmel, H. J.; Downs, A. J.; Greene, T. M. *Chem. Rev.* **2002**, *102*, 4191.

(39) Darling, J. H.; Ogden, J. S. *J. Chem. Soc., Dalton Trans.* **1972**, 2496.

JP9010422